Electronic Supplementary Material (ESI) for Catalysis Science & Technology.

Supplementary Information

On the role of the alkali on the synthesis of methanethiol via methanol thiolation

Ricardo Bermejo-Deval, Raimund M. H. Walter, Oliver Y. Gutiérrez,*§ and Johannes A. Lercher*

Technische Universität München, Department of Chemistry, Catalysis Research Center, Lichtenbergstraße 4, 85748 Garching (Germany)

§ Present address: Institute for Integrated Catalysis, Pacific Northwest National Laboratory, Richland, Washington 99354, United States

* Corresponding authors. Fax: +49 89 28913544.

oliver.gutierrezTinoco@pnnl.gov (O.Y. Gutiérrez)

johannes.lercher@ch.tum.de (J.A. Lercher)

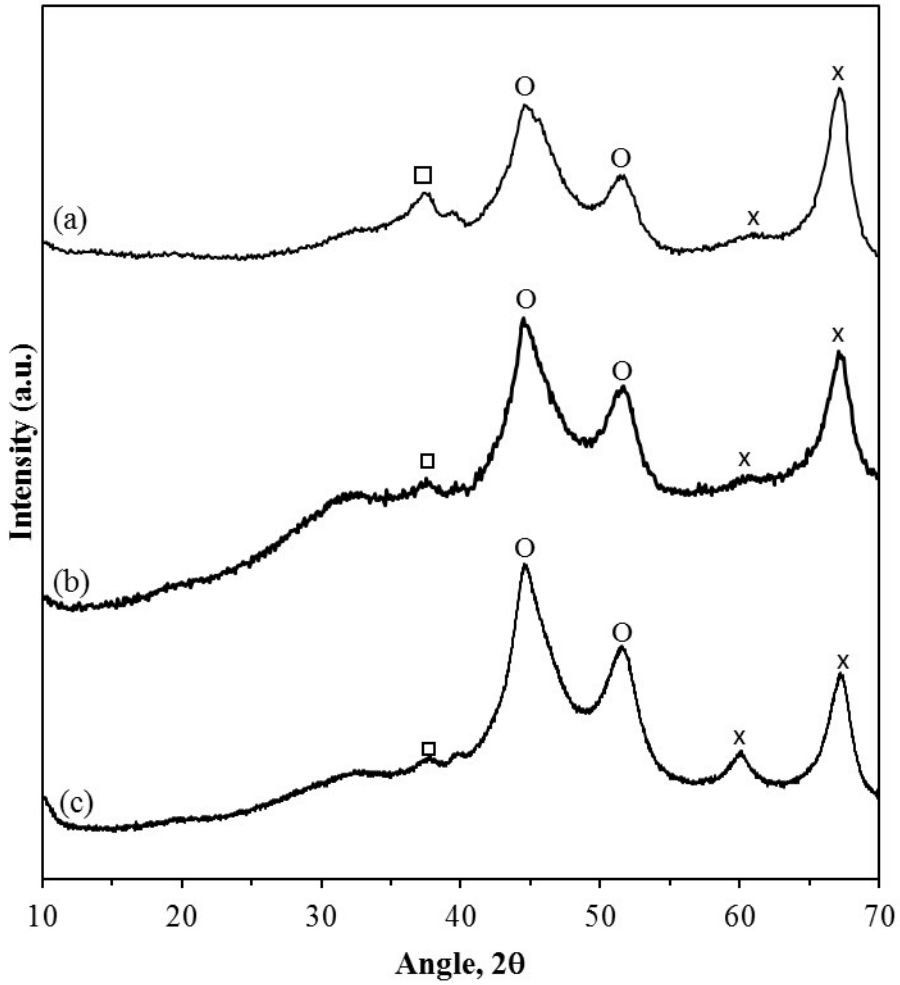

Figure S1 X-ray diffraction of a) K/Al_2O_3, b) Rb/Al_2O_3 and c) Cs/Al_2O_3 prior sulfidation. The symbols represent: x γ-Al_2O_3, O K_2CO_3, Rb_2CO_3 or Cs_2CO_3, and □ corundum.

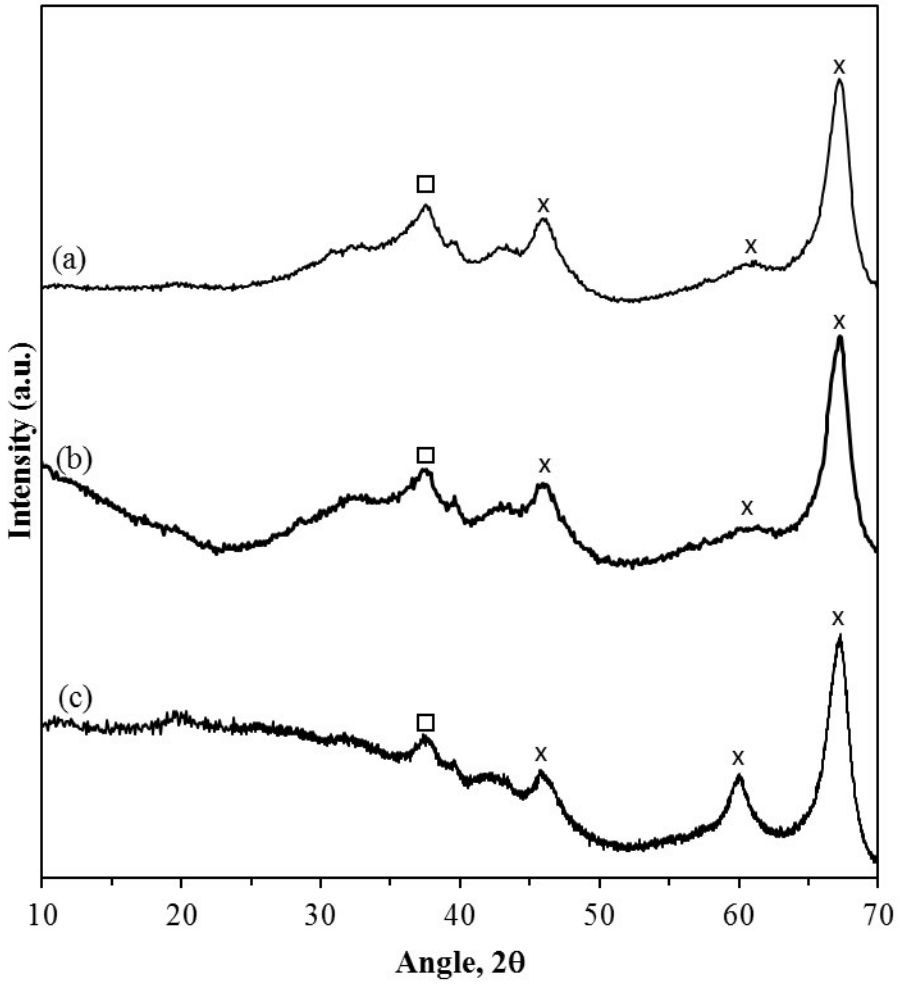

Figure S2 X-ray diffraction of a) K/Al_2O_3, b) Rb/Al_2O_3 and c) Cs/Al_2O_3 after sulfidation. The symbols represent: x γ-Al_2O_3 and ■ corundum.

Table S1 Raman shifts and assignments from the different sulfur anions[1–3].

Anion	Raman Shift (cm^{-1})	Assignment
Sulfite (SO_3^{-2})	496	(E) Antisymmetric SO_3 deformation
Sulfite (SO_3^{-2})	647	(A_1) Symmetric SO_3 deformation
Sulfite (SO_3^{-2})	986	(E) Antisymmetric SO_3 stretching
Thiosulfate ($S_2O_3^{-2}$)	323	(E) Symmetric S-S-O deformation
Thiosulfate ($S_2O_3^{-2}$)	452	(A_1) Symmetric SO_3 deformation
Thiosulfate ($S_2O_3^{-2}$)	656	(A_1) Symmetric S-SO_3 stretching
Thiosulfate ($S_2O_3^{-2}$)	1016	(A_1) Symmetric SO_3 stretching
Dithionate ($S_2O_6^{-2}$)	204	(E_u) Symmetric SO_3 deformation
Dithionate ($S_2O_6^{-2}$)	1000	(A_{2u}) Symmetric stretching
Pyrolsulfite ($S_2O_5^{-2}$)	660	(A_1) Symmetric SO_3 deformation
Pyrolsulfite ($S_2O_5^{-2}$)	1050	(A_1) Symmetric SO_3 stretching
Sulfate (SO_4^{-2})	450	(A_1) Symmetric SO_4 stretching
Sulfate (SO_4^{-2})	983	(E) Antisymmetric SO_4 stretching

1) $K_2CO_3 + 2H_2O + H_2S \rightleftharpoons K_2SO_3 + CO_2 + 3H_2$ $K_{eq} = 6.76 \cdot 10^{-9}$

2) $K_2SO_3 + H_2O \rightleftharpoons K_2SO_4 + H_2$ $K_{eq} = 4.88 \cdot 10^{2}$

3) $K_2SO_3 + H_2S \rightleftharpoons K_2S_2O_3 + H_2$ $K_{eq} = 1.64$

4) $K_2O + H_2S \rightleftharpoons K_2S + H_2O$ $K_{eq} = 2.34 \cdot 10^{18}$

Figure S3. Plausible reactions yielding sulfur oxyanions and the corresponding equilibrium constants at 400 °C and 1 atm. The equilibrium constants were calculated with the HSC-chemistry software. The decomposition of K_2CO_3 into K_2SO_3 and CO_2 would be driven, under flow conditions, by the continuous removal of CO_2 and H_2 from the system shifting the equilibrium towards the product side.

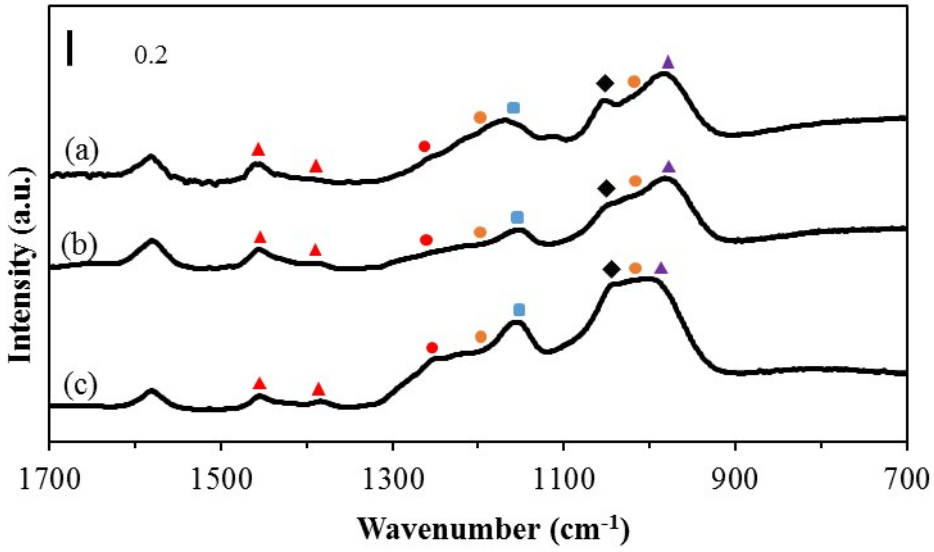

Figure S4. Infrared spectroscopy in a) K/Al_2O_3-H_2S, b) Rb/Al_2O_3-H_2S and c) Cs/Al_2O_3-H_2S. The symbols represent the anions: sulfate (red dot), thiosulfate (blue square), dithionate (black diamond), pyrosulfite (orange dot), pyrosulfate (red triangle) and sulfite (purple triangle).

Table S2 Infra-red bands and assignments from the different sulfur anions.[1,2,4]

Anion	IR band (cm^{-1})	Assignment
Sulfite (SO_3^{-2})	968	(A_1) Symmetric SO_3 stretching
Thiosulfate ($S_2O_3^{-2}$)	1146	(E) Antisymmetric SO_3 stretching
Dithionate ($S_2O_6^{-2}$)	1000	(A_{2u}) Symmetric stretching
Pyrolsulfite ($S_2O_5^{-2}$)	970	(A_2) Symmetric SO_2 stretching
Pyrolsulfite ($S_2O_5^{-2}$)	1196	(A_2) Symmetric SO_3 stretching
Pyrosulfate ($S_2O_7^{-2}$)	1380	--
Pyrosulfate ($S_2O_7^{-2}$)	1450	--

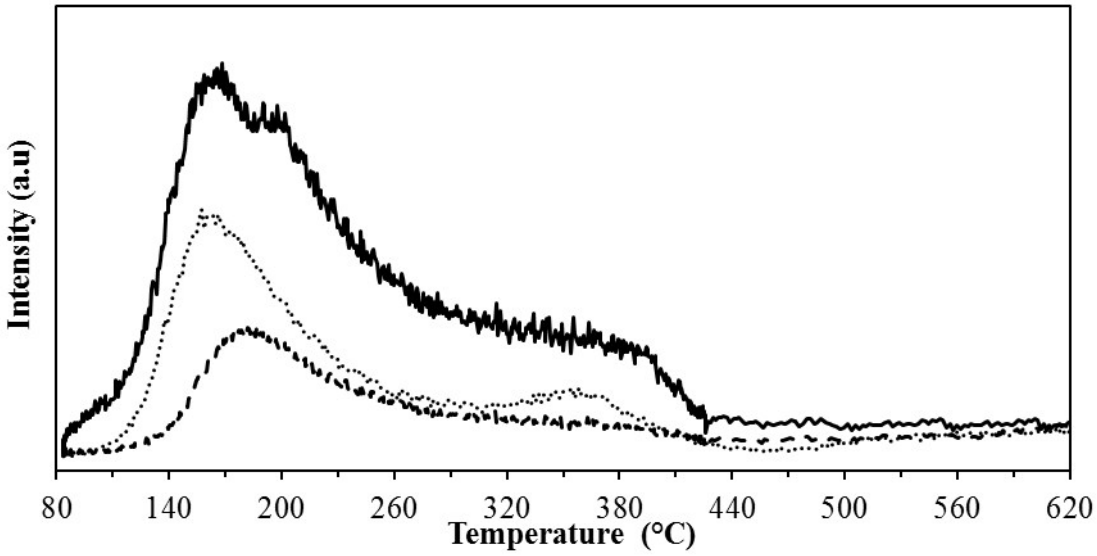

Figure S5 CO_2 desorption for catalysts K/Al_2O_3-H_2S(--),Rb/Al_2O_3-H_2S(··) and Cs/Al_2O_3-H_2S(–).

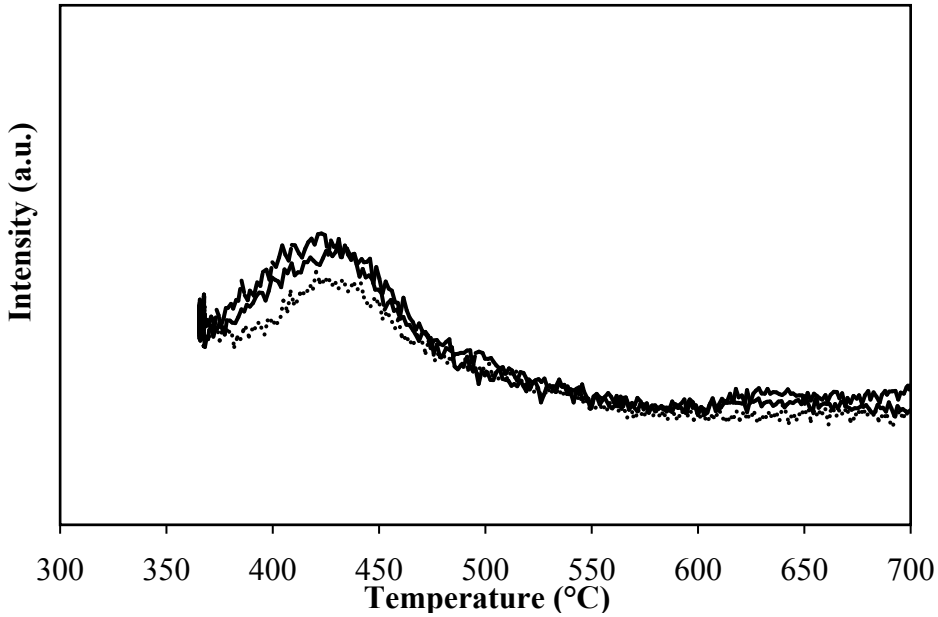

Figure S6 CH_3OH desorption profiles from K/Al_2O_3-H_2S(--), Rb/Al_2O_3-H_2S(··) and Cs/Al_2O_3-H_2S(–).

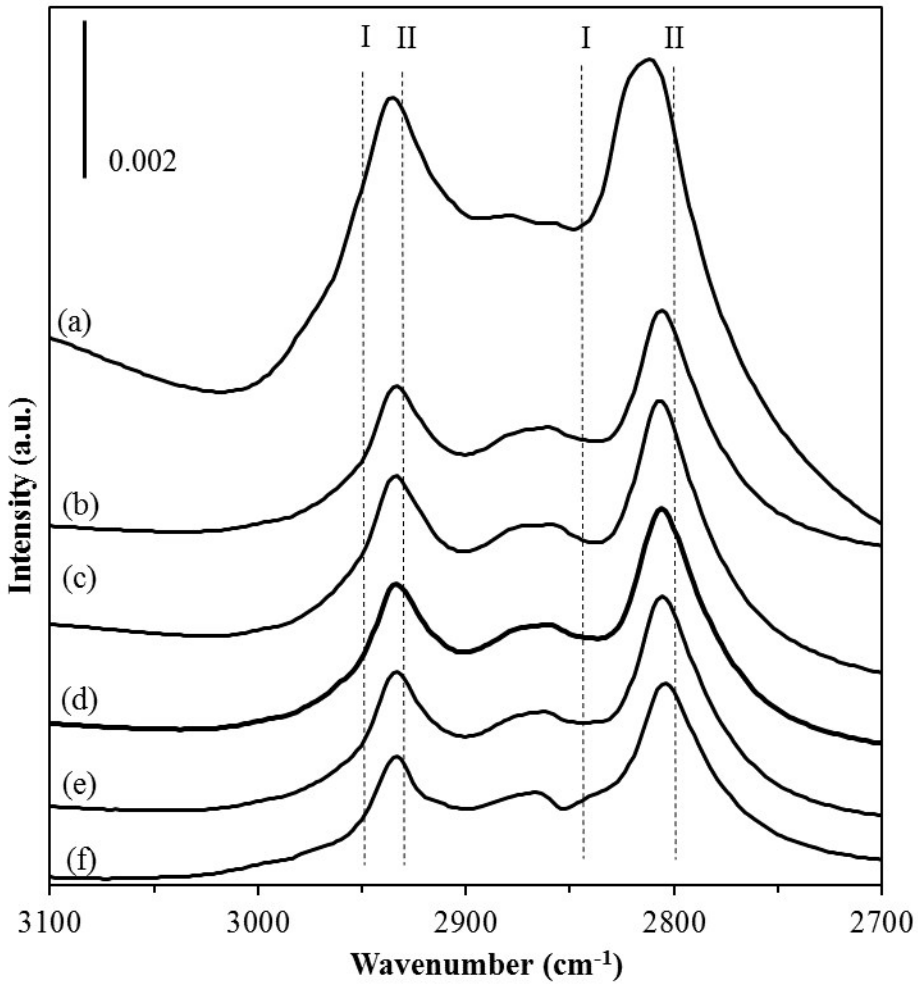

Figure S7 IR Spectra of methanol adsorbed on K/Al_2O_3-H_2S at a) 0.5 mbar and 50 °C, b) 0.1 mbar and 50 ºC, c) after evacuation at 50 °C, d) after evacuation at 100ºC, e) after evacuation at 150 ºC and f) after evacuation at 300ºC.

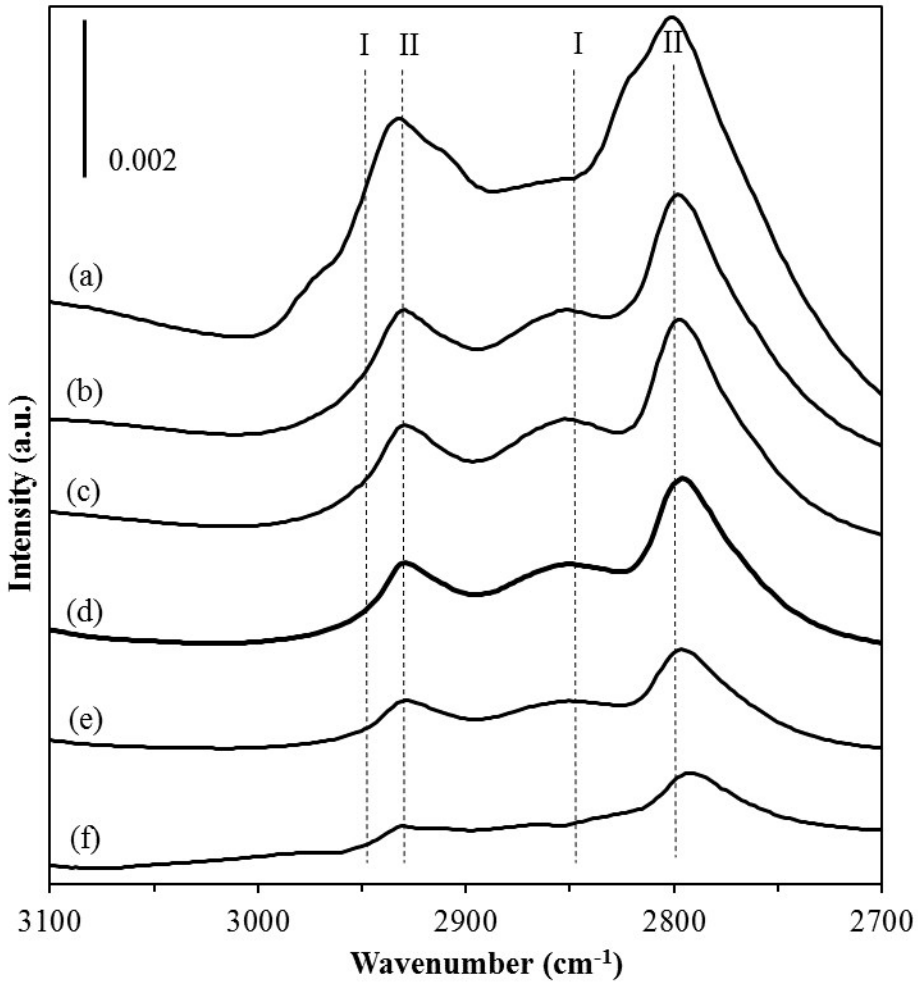

Figure S8 IR Spectra of methanol adsorbed on Rb/Al_2O_3-H_2S at a) 0.5 mbar and 50 °C, b) 0.1 mbar and 50 ºC, c) after evacuation at 50 °C, d) after evacuation at 100ºC, e) after evacuation at 150 ºC and f) after evacuation at 300ºC.

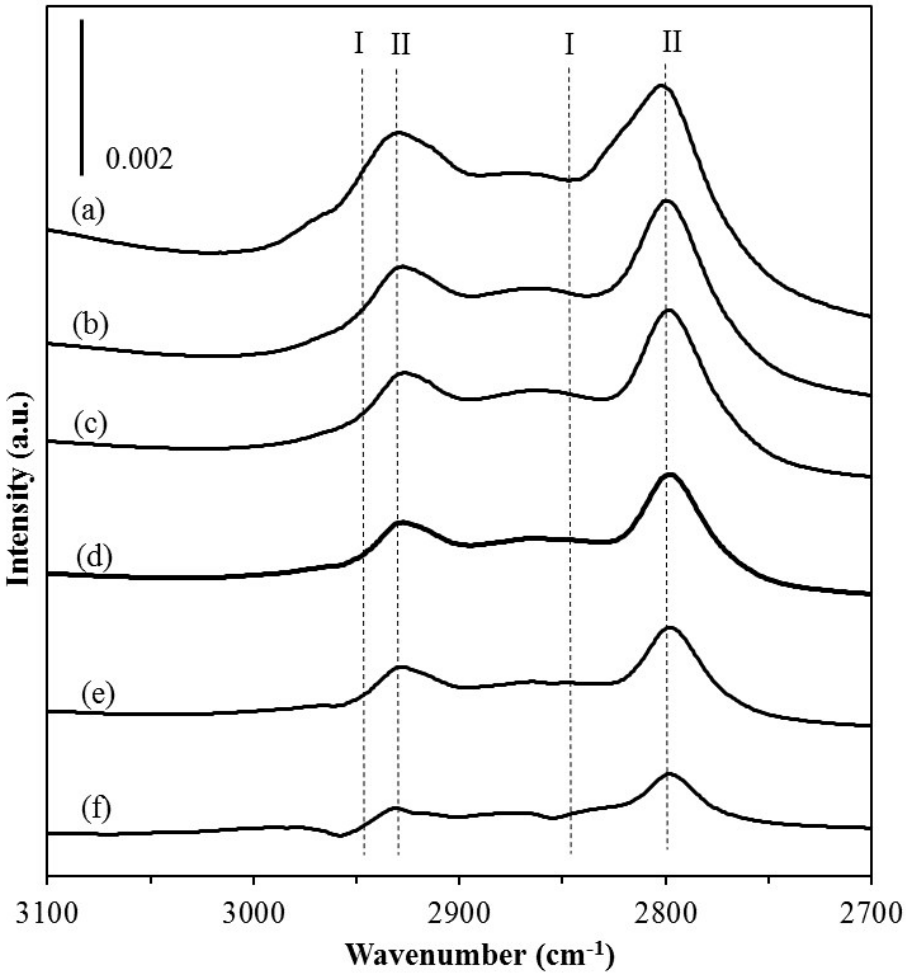

Figure S9 IR Spectra of methanol adsorbed on Cs/Al_2O_3-H_2S at a) 0.5 mbar and 50 °C, b) 0.1 mbar and 50 ºC, c) after evacuation at 50 °C, d) after evacuation at 100ºC, e) after evacuation at 150 ºC and f) after evacuation at 300ºC.

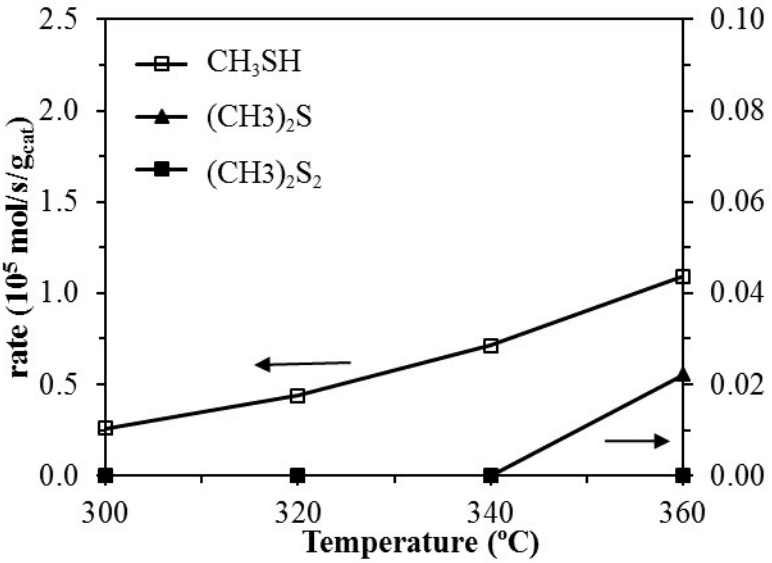

Figure S10 Product rates during the reaction of methanol and H_2S over K/Al_2O_3-H_2S ($1.3 \cdot 10^{-3}$ mol/g Al_2O_3) at varying temperatures.

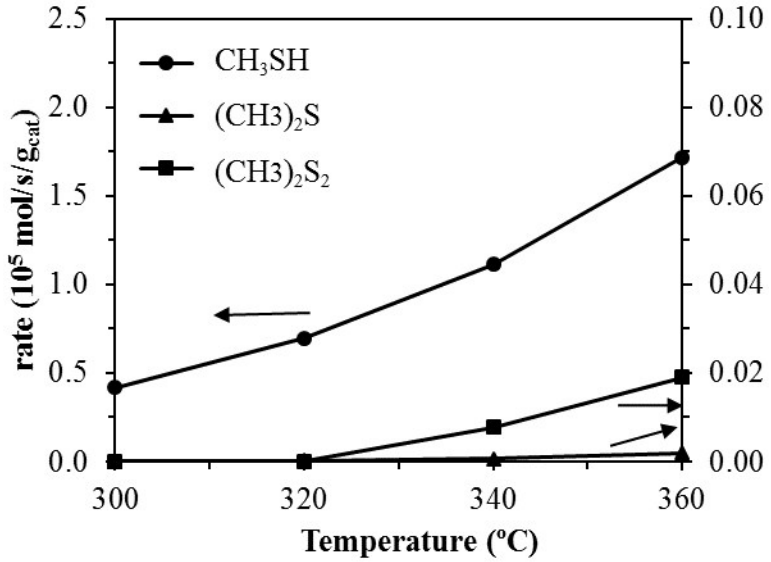

Figure S11 Product rates during the reaction of methanol and H_2S over Rb/Al_2O_3-H_2S ($1.5 \cdot 10^{-3}$ mol/g Al_2O_3) at varying temperatures.

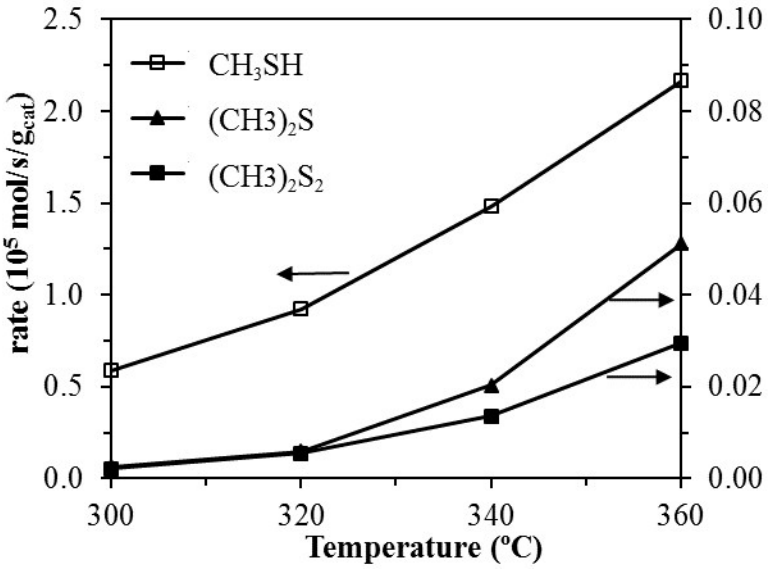

Figure S12 Product rates during the reaction of methanol and H_2S over Cs/Al_2O_3-H_2S ($1.5 \cdot 10^{-3}$ mol/g Al_2O_3) at varying temperatures.

Analysis of kinetic data

Conversion (*X*), yield(*Y*) and selectivity(*S*) are always referred to the concentration of methanol:

$$X_{CH_3OH}(\%) = \frac{C_{CH_3OH_0} - C_{CH_3OH}}{C_{CH_3OH_0}}$$

$$Y_i(\%) = \frac{C_i}{C_{CH_3OH_0}} \left| \frac{\mu_{CH_3OH}}{\mu_i} \right|$$

$$S_i(\%) = \frac{C_i}{C_{CH_3OH_0} - C_{CH_3OH}} \left| \frac{\mu_{CH_3OH}}{\mu_i} \right|$$

The apparent activation energies were calculated from a semilogarithmic plot of Ln k vs 1/T, using the Arrhenius equation:

$$k = A \cdot \exp(-E_a/RT)$$

Where E_a is the apparent activation energy (kJ/mol), A is the pre-exponential factor, R is the molar gas constant (R = 8.314 J/(mol·K), and T is the absolute temperature (K).

Table S3 First-order apparent rate constants (mol s^{-1} g_{cat}^{-1}) with respect to methanol in between temperatures of 300-360ºC, 9 bar and 2:1 of H_2S:CH_3OH.

	Temperature (ºC)			
Catalyst	300	320	340	360
K/Al_2O_3-H_2S	$1.75 \cdot 10^{-5}$	$8.73 \cdot 10^{-6}$	$4.77 \cdot 10^{-6}$	$1.86 \cdot 10^{-6}$
Rb/Al_2O_3-H_2S	$1.96 \cdot 10^{-5}$	$1.13 \cdot 10^{-5}$	$4.51 \cdot 10^{-6}$	$2.58 \cdot 10^{-6}$
Cs/Al_2O_3-H_2S	$3.64 \cdot 10^{-5}$	$2.07 \cdot 10^{-5}$	$1.25 \cdot 10^{-5}$	$6.53 \cdot 10^{-6}$

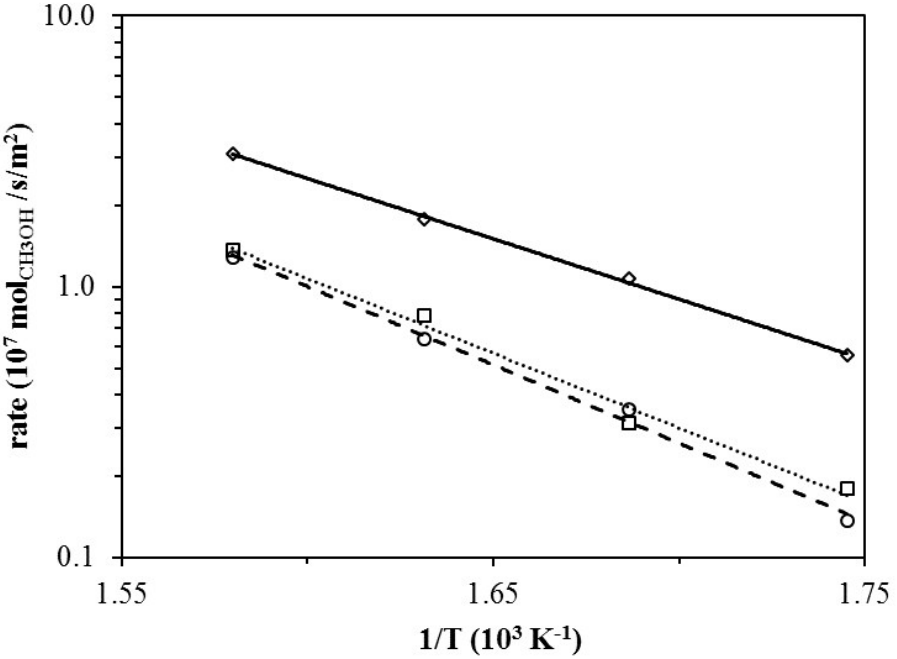

Figure S13 The Arrhenius plot of the first-order apparent rate constants with respect to methanol and normalized m^2 in between temperatures of 300-360ºC, 9 bar and 2:1 of H_2S:CH_3OH, being K/Al_2O_3-H_2S(--, circles), Rb/Al_2O_3-H_2S(··, squares) and Cs/Al_2O_3-H_2S(–, diamond).

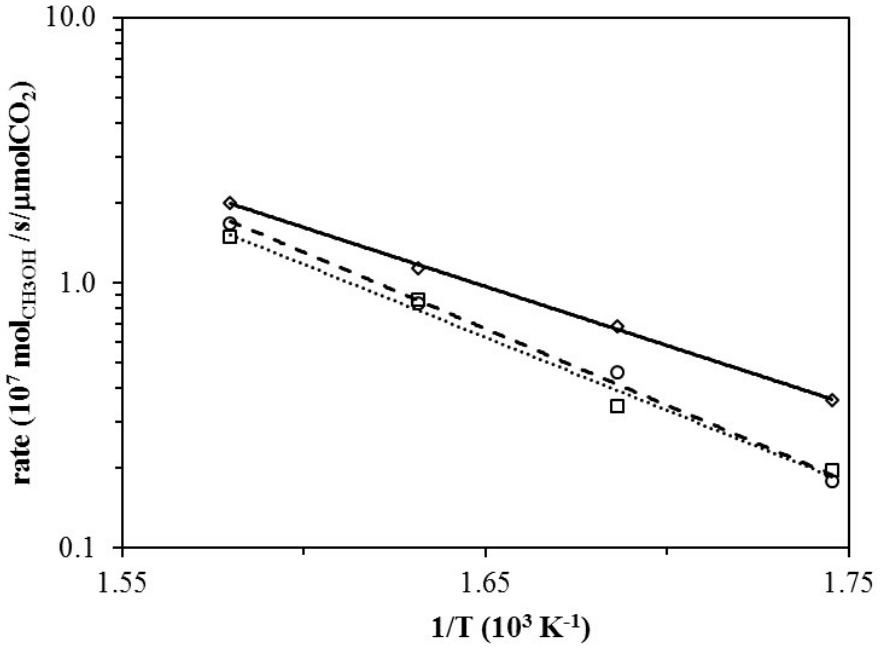

Figure S14 The Arrhenius plot of the first-order apparent rate constants with respect to methanol and normalized per µmol CO_2 in between temperatures of 300-360ºC, 9 bar and 2:1 of H_2S:CH_3OH, being K/Al_2O_3-H_2S(--, circles), Rb/Al_2O_3-H_2S(··, squares) and Cs/Al_2O_3-H_2S(–, diamond).

References

(1) Church, J. S.; Evans, D. J. *Spectrochim. Acta. A. Mol. Biomol. Spectrosc.* **2008**, *69* (1), 256.

(2) Takahashi, H.; Kaneko, N.; Miwa, K. *Spectroquimica Acta* **1982**, *38* (11), 1147.

(3) Jayaraman, K.; Choudhury, A.; Rao, C. N. R. *Solid State Sci.* **2002**, *4* (3), 413.

(4) Hoshi, N.; Sakurada, A.; Nakamura, S.; Hori, Y. *J. Phys. Chem. B* **2002**, *106* (2), 1985.